Supplemental Materials

Molecular Biology of the Cell

Aguilar et al.

Supplementary Figure Legends

Figure S1. αTat1, the major K40 α-tubulin acetyltransferase *in vivo*, is dispensable for mammalian development and ciliogenesis. (A) Upper: 11 out of the 13 exons of *αTat1* were replaced by a neo resistance cassette to generate the *αTat1*$^{-/-}$ allele. Lower: PCR genotyping of *αTat1*$^{+/+}$, *αTat1*$^{-/-}$ and *αTat1*$^{+/-}$ mice with primers P1, P2 and P3 indicated in the upper panel. (B) K40 acetylated α-tubulin immunostaining (green) of adult brain cryosections of *αTat1*$^{+/+}$ and *αTat1*$^{-/-}$ mice. No K40 acetylated α-tubulin staining was detected in *αTat1*$^{-/-}$ brain sections, especially in the cerebellum and the hippocampus, two regions that show high levels of staining in wild-type animals. ML, molecular layer; PCL, Purkinje cell layer; GCL, granule cell layer; sr, stratum radiatum: sp, stratum pyramidale. (C) *αTat1*$^{+/+}$ and *αTat1*$^{-/-}$ MEFs, were immunostained for K40 acetylated α-tubulin (green). Interphase *αTat1*$^{-/-}$ MEFs are devoid of K40 acetylated α-tubulin. (D) Weight curves of two litters (7 pups and 11 pups, respectively). No difference in weight gain was observed between wild-type (black line) or heterozygous (dashed line) and *αTat1*$^{-/-}$ (grey line) pups. (E) Hematoxylin and Eosine staining of adult *αTat1*$^{+/+}$ and *αTat1*$^{-/-}$ brain sagittal sections. Aside from an enlargement of the superior blade of the granular layer in the dentate gyrus (black arrow), the global brain anatomy was conserved in *αTat1*$^{-/-}$ mice. (Scale bars: B, 50 µm; C, 20 µm; E, 1mm (left), 500 µm (right)).

Figure S2. αTat1 is not required for highly acetylated tissues morphogenesis. (A) ZO1 (green), K40 acetylated (red) and detyrosinated (green) α-tubulin whole mount immunostaining of corneal endothelium. Wild-type corneal endothelial cells present a stereotypical epithelial monolayer organization and a perinuclear ring of acetylated and detyrosinated microtubules (arrows). In *αTat1*$^{-/-}$ corneal endothelia, the epithelial organization (hexagonal cell shape, homogeneous cell size, equidistant nuclei spacement) and the presence of the detyrosinated α-tubulin ring were conserved. (B) Auditory brainstem responses (ABR) and distortion product of otoacoustic emission (DPOAE) thresholds were measured for *αTat1*$^{-/-}$ (red, n=3), *αTat*$^{+/-}$ (blue, n= 2)

and wildtype (black, n=1) mice at P28. All tested mice had normal hearing thresholds. Data is presented as mean± SEM. (Scale bars: 30 µm (top), 10 µm (bottom)).

Figure S3. α-tubulin tyrosination/detyrosination cycle, Purkinje cells dendritogenesis and axonal morphology are not affected in the absence of αTat1. (A) *αTat1*$^{+/+}$ and *αTat1*$^{-/-}$ adult brain cryosections were immunostained for tyrosinated (Tyr-Tub, dynamic microtubules) and detyrosinated α-tubulin (Detyr-Tub, long-lived microtubules). The spatial organization of both types of microtubules, here shown in the cerebellar cortex and the hippocampus, was conserved in the *αTat1*$^{-/-}$ mice. In particular, the cytoskeletal architecture of the cerebellar Bergman glia, labeled with glial fibrillary acidic protein (GFAP) and S100β (red), was unchanged in the αTat1 deficient cerebellum. ML, molecular layer; PCL, Purkinje cell layer; GCL, granule cell layer; so = stratum oriens, sp = stratum pyramidale, sr stratum radiatum, CA, cornu ammonis. (B) Polyglutamylated α-tubulin immunostaining (GT335 antibody, green) of *αTat1*$^{+/+}$ and *αTat1*$^{-/-}$ adult brain cryosections. The organization of the dendritic tree of the Purkinje cells is conserved in the *αTat1*$^{-/-}$ cerebellum. In the corpus callosum, the polyglutamylated α-tubulin staining (white) shows the absence of morphological defects in axonal tracts and individual axons (arrows) in *αTat1*-deficient mice. (Scale bars: A, 50 µm (cerebellum, hippocampus bottom), 100 µm (hippocampus top); B, 20 µm (cerebellum), 10 µm (corpus callosum)).

Figure S4. αTat1 is required for contact inhibition. (A) *αTat1*$^{+/+}$, *αTat1*$^{-/-}$ and *αTat1*$^{-/-}$ cells expressing GFP, GFP-αTAT1 or GFP-αTAT1[D157N] were seeded at 15,000 cells/cm^2. The day after seeding, cells were fixed, immunostained for ZO-1 (red) and imaged in a Z-stack. Nuclei were labeled with Hoechst (blue). (B) K40 acetylated α-tubulin (red) and GFP (green) immunostaining of all studied cell lines (*αTat1*$^{+/+}$, *αTat1*$^{-/-}$ and *αTat1*$^{-/-}$ cells expressing GFP, GFP-αTAT1 or GFP-αTAT1[D157N]). Only GFP-αTAT1 restores K40 α-tubulin acetylation to near wild-type levels. (C) WT and *αTat1*$^{-/-}$ cells were seeded at low density in order to assess Merlin localization in cells that do not contact any other cell and stained for Merlin (green), total (red) and acetylated (white) α- tubulin. (D) *αTat1*$^{-/-}$ cells expressing GFP (red), GFP-αTAT1 (blue) or GFP-αTAT1[D157N] (orange) were analyzed by flow cytometry to assess their relative size. Histogram shows the forward scatter (FSC-A) for each cell line. (Scale bars: B, 20 µm, C, 10 µm).

Figure S5. αTat1 is required for cell adhesion. Shorter exposure and larger pictures of the experiment shown in Figure 4D. *αTat1*$^{+/+}$ and *αTat1*$^{-/-}$ cells were treated with nocodazole or blebbistatin and immunostained for α-tubulin (red). Actin was labeled using Alexa488-Phalloidin (green). While nocodazole treatment stimulates fiber stress formation in wild-type cells, no or few stress fibers were observed in *αTat1*$^{-/-}$ cells, which rounded up and detached. In blebbistatin-treated wild-type cells, the inhibition of myosin II function induces cytoplasmic collapse. In *αTat1*$^{-/-}$ cells, blebbistatin treatment did not yield any major morphological alteration. (Scale bar: 30 µm)

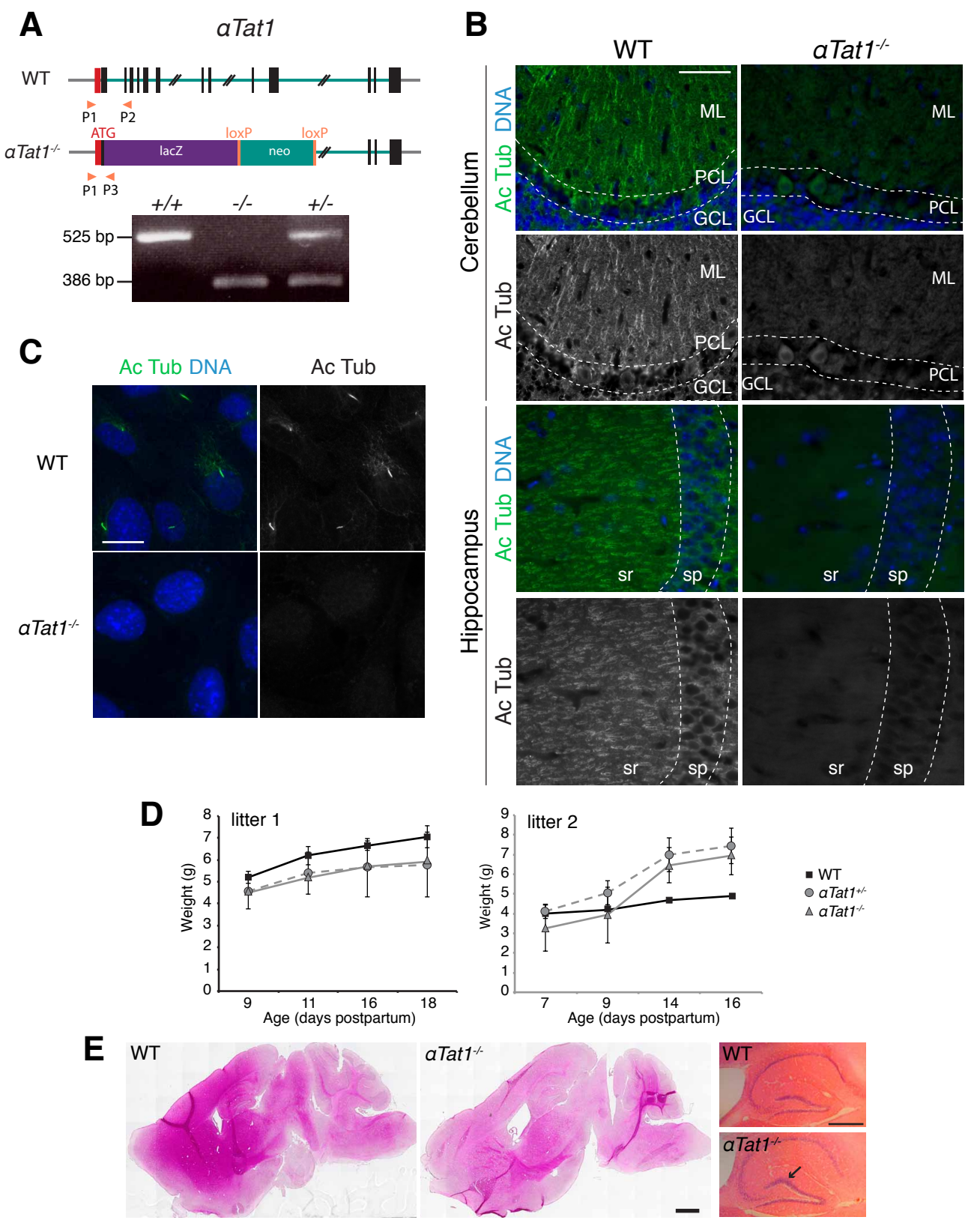

Aguilar et al., Figure S1

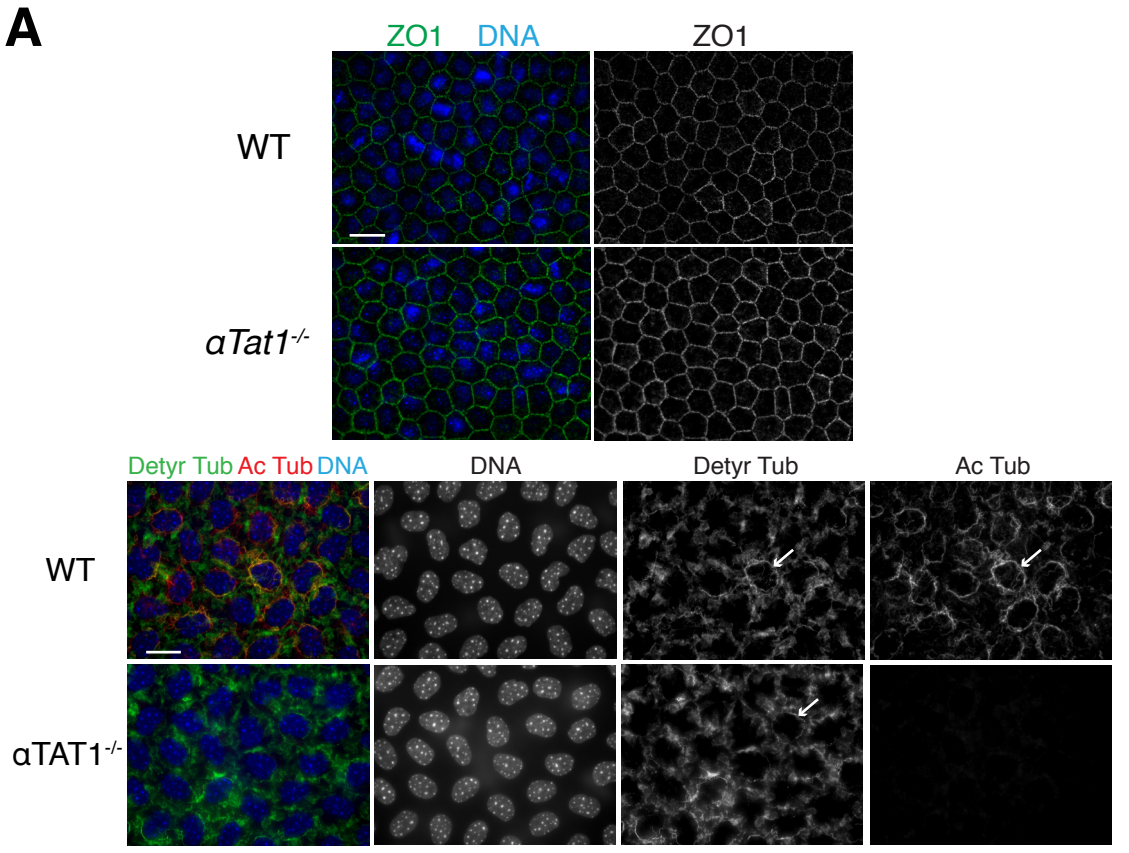

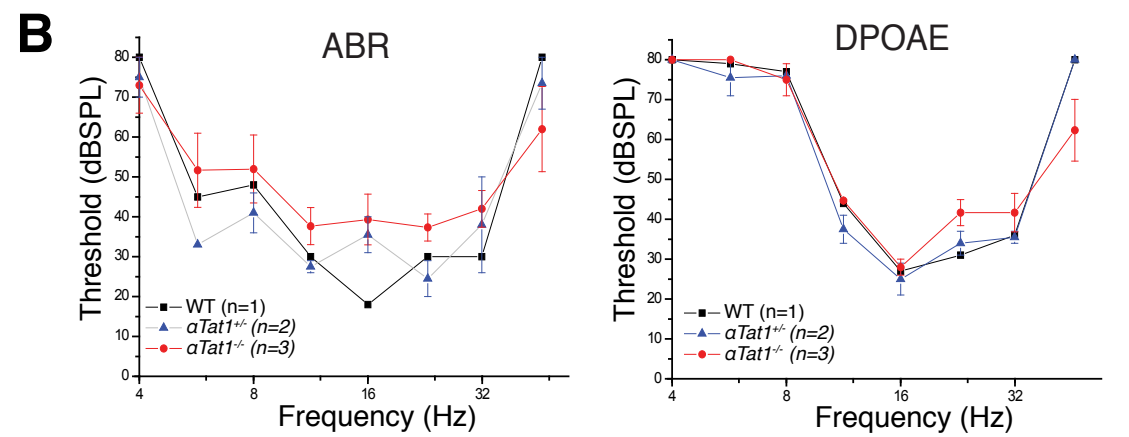

Aguilar et al., Figure S2

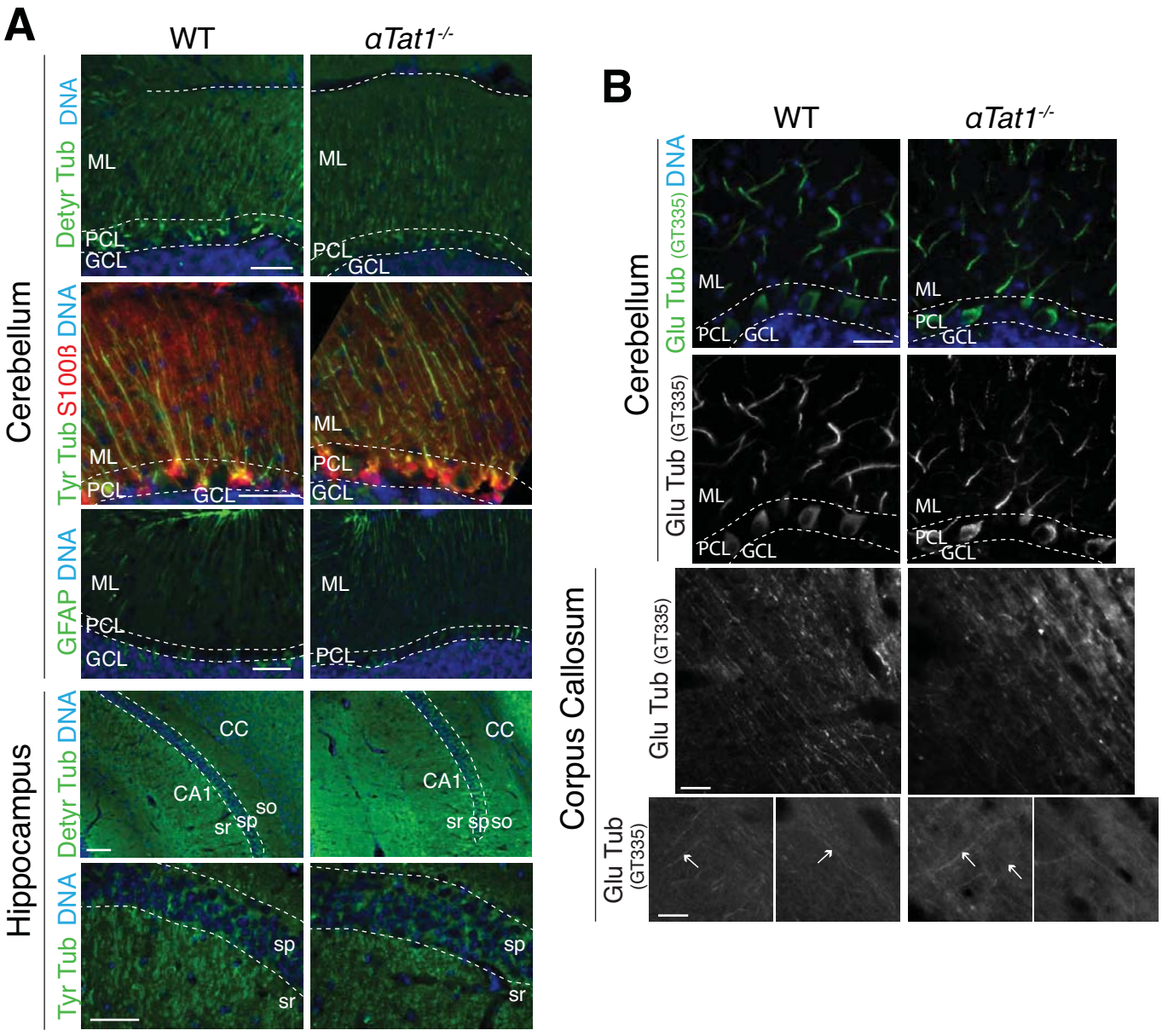

Aguilar et al., Figure S3

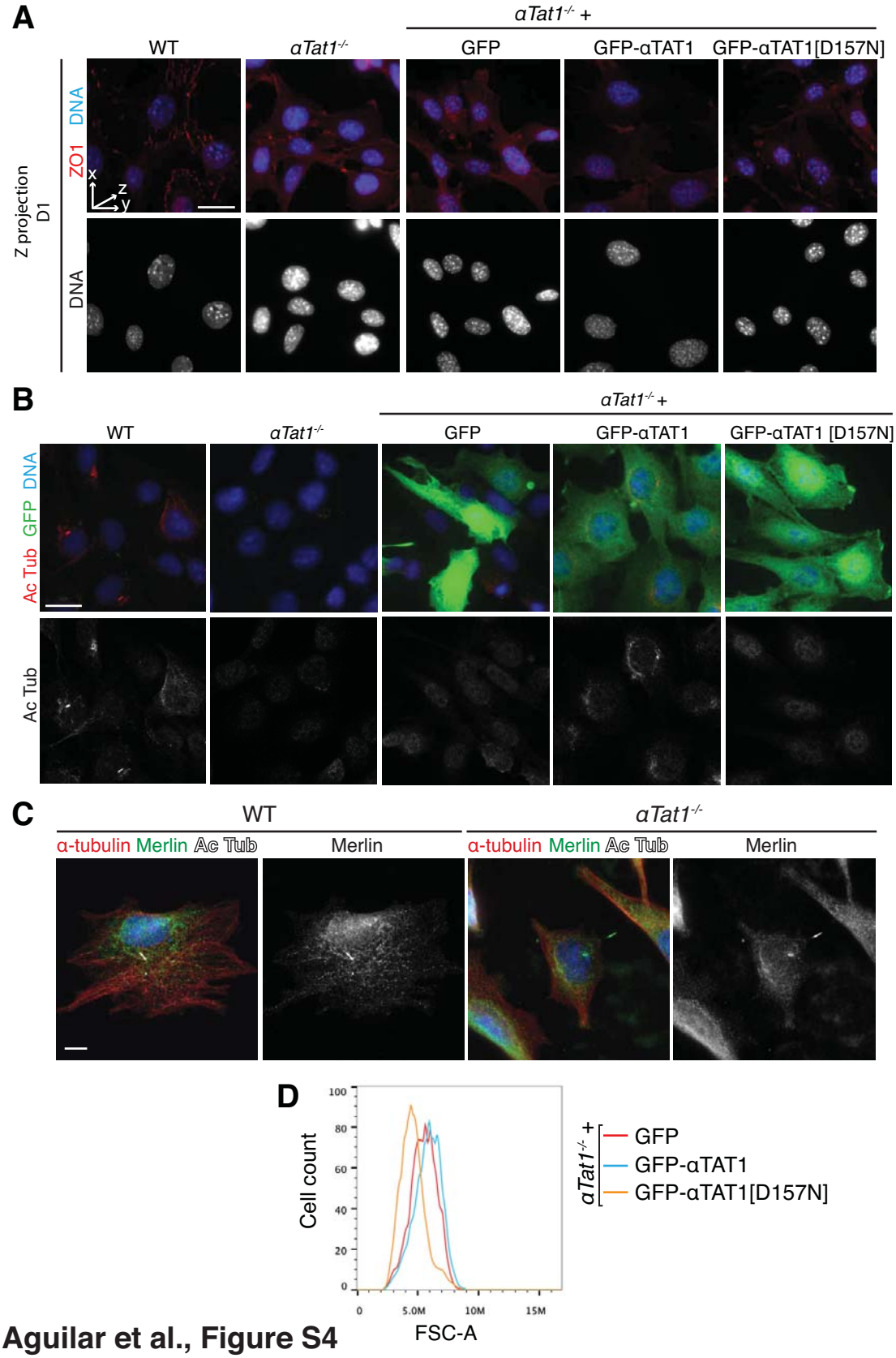

Aguilar et al., Figure S4

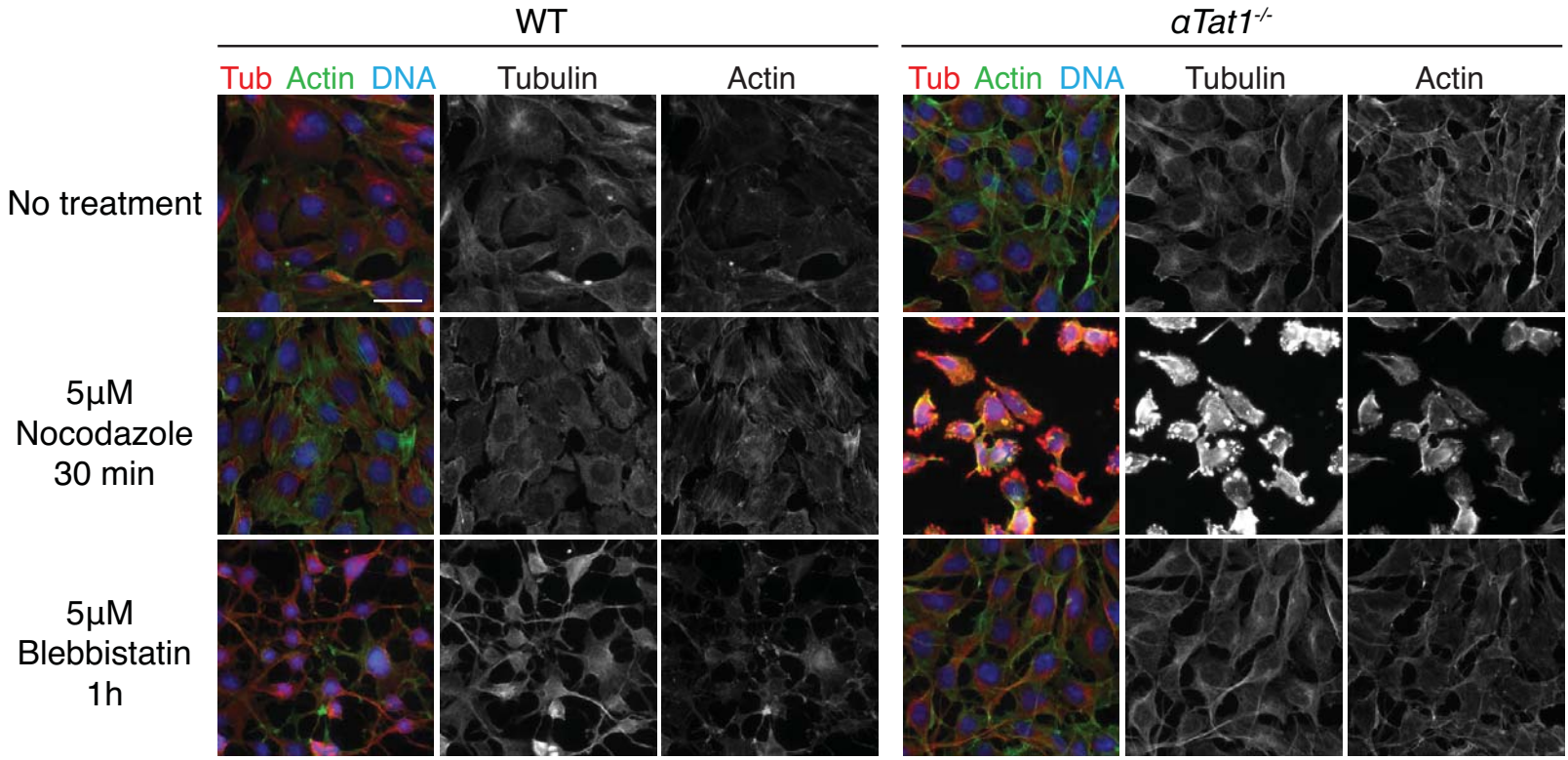

Aguilar et al., Figure S5